Journal of Statistical Physics, Vol. 3, No. 3, 1971

Stochasticity in Many-Dimensional Nonlinear Oscillating Systems

B. V. Chirikov,[1] E. Keil,[2] and A. M. Sessler[3]

Received November 11, 1970; revised February 4, 1971

Qualitative analytic estimates of the stochasticity limit of one- and many-dimensional nonlinear oscillating systems are derived using the overlapping of first-order resonances as a criterion for stochasticity. Computational results obtained with several very simple transformations are compared with the analytic estimates. Numerical studies significantly below the stochasticity limit of a many-dimensional nonlinear system reveal an example of a very slow instability, the first, to the best of our knowledge.

KEY WORDS: Stochasticity limit; nonlinear oscillators; overlapping of resonances; nonlinear transformations; slow instability.

1. INTRODUCTION

Motivated by the very important question of long-term stability of particle beams in storage rings, we study in this paper some mathematical models, namely nonlinear transformations, which replicate the essential elements determining the dynamical behavior of particle motion in a storage ring.

In Sections 2–4, qualitative analytic estimates of the stochasticity limit of one- and many-dimensional nonlinear oscillating systems are derived using the overlapping of first-order resonances as a criterion for stochasticity. Computational results obtained with several very simple transformations are compared with the analytic estimates.

The stochasticity limit, with instability above it and apparent stability below it, affords a gross description of the behavior of stored particles. Especially for protons and antiprotons, where radiation damping is negligibly small, it is important to ascertain whether or not motion below the stochasticity limit is truly stable. In

[1] Institute of Nuclear Physics, Novosibirsk, USSR.
[2] ISR Division, CERN, Geneva, Switzerland.
[3] Lawrence Radiation Laboratory, Berkeley, California.

Section 5, we present a numerical example of a very slow instability below the stochasticity limit of a many-dimensional nonlinear system.

2. ANALYTIC ESTIMATE OF THE STOCHASTICITY LIMIT

2.1. Equations of Motion

Consider the following canonical equations for a many-dimensional nonlinear oscillating system:

$$\dot{I} = \epsilon f(I, \theta, t), \qquad \dot{\theta} = \omega(I) + \epsilon\phi(I, \theta, t) \tag{1}$$

Here, I and θ are N-dimensional vectors of momenta and phases, respectively, and ϵ is a small perturbation parameter.

The unperturbed motion with $\epsilon = 0$ is of maximum stability (it possesses all N motion integrals $I = \text{const}$). The problem to be studied is the qualitative behavior of the perturbed motion with $\epsilon \neq 0$.

In the zeroth approximation ($\epsilon = 0$) the system (1) has the following solution:

$$I = \text{const}, \qquad \theta = \omega(I)t \tag{2}$$

2.2. Resonances

We expand the first equation of (1) in a multiple Fourier series

$$\dot{I} = \epsilon \sum_{mn} f_{mn}(I) \exp(in\theta + im\kappa) \tag{3}$$

Introducing $\Omega = 2\pi/T$, where T is the period of the external perturbation, and substituting the solution (2) into the right-hand side, we find the following new set of equations:

$$\begin{aligned} \dot{I} &= \epsilon \sum_{mn} f_{mn}(I) \exp(in\theta + im\kappa) \\ \dot{\theta} &= \omega(I), \qquad \dot{\kappa} = \Omega. \end{aligned} \tag{4}$$

We have neglected the second term in the equation for $\dot{\theta}$, Eq. (1). This is a good approximation if the nonlinearity coefficient is not small[1]:

$$\alpha = |(I/\omega)\, \partial\omega/\partial I| \gg \epsilon \tag{5}$$

The opposite case is considered in Section 3.3.

2.3. Resonance Width

For sufficiently small perturbations ϵ, only resonant conditions can have an important influence on the motion. In this case, the phase $\psi_{mn} = n\theta + m\kappa$ is a slow

variable. The phase oscillation equation for this isolated resonance can be found by combining Eqs. (4):

$$\begin{aligned} \dot{\psi}_{mn} &= n\dot{\theta} + m\dot{\kappa} = n\dot{\theta} = n\, d\omega(I)/dt = n(\partial\omega/\partial I)\dot{I} \\ \ddot{\psi}_{mn} &= n\epsilon(\partial\omega/\partial I) f_{mn}(I) \exp(i\psi_{mn}) \end{aligned} \tag{6}$$

Taking the real part of this expression,

$$\ddot{\psi}_{mn} = n\epsilon(\partial\omega/\partial I) f_{mn}(I) \cos \psi_{mn} \tag{7}$$

and linearizing it in the vicinity of a fixed point, we obtain the following frequency for small amplitude oscillations:

$$\Omega_{mn}^2 = n\epsilon(\partial\omega/\partial I) f_{mn}(I) \tag{8}$$

It may be seen that (7) can be derived from the following Hamiltonian:

$$\mathscr{H} = \tfrac{1}{2}\dot{\psi}_{mn}^2 - \Omega_{mn}^2 \sin \psi_{mn} \tag{9}$$

This allows us to calculate over what range of frequencies $\Delta\omega$ the motion will lock onto the resonance, by comparing $\dot{\psi}_{mn}$ to the depth of the potential well. We find

$$n\,\Delta\omega = 2\dot{\psi}_{mn} = 4\Omega_{mn} \tag{10}$$

2.4. Overlapping of Resonances

It is well confirmed[2] that there occurs a strong instability with randomlike motion when many resonances overlap. The earliest indication for such an instability was probably found by Goward[3] and Hine.[3a] As an estimate for the stochasticity limit, we adopt the condition of resonance overlapping. The main difficulty is connected with the high-order resonances [the approximations following after (4)], where the question arises whether the contribution of high-order resonances is essential for the overlapping condition. We base our estimates on the hypothesis that it is sufficient to take into account only first-order resonances according to (4) and that the influence of all higher-order approximations can be neglected.

Consider first the one-dimensional case. From the resonance condition

$$n\omega + m\Omega = 0 \tag{11}$$

one can see that the number of resonances for a given harmonic number n and for a frequency interval of unity is proportional to n:

$$N_r \propto n \tag{12}$$

Overlapping of resonances means that the sum of the widths of all resonances with density (12) is greater than one. Hence, we find for the stochasticity limit

$$1 \sim \sum_n n(\Delta\omega) = 2\epsilon^{1/2} \sum_n (n f_n\, \partial\omega/\partial I)^{1/2} \tag{13}$$

Replacing the sum by an integral and solving for ϵ, we have

$$\epsilon \sim \tfrac{1}{4}\left[\int_1^\infty (nf_n\, \partial\omega/\partial I)^{1/2}\, dn\right]^{-2} \tag{14}$$

If $\epsilon \approx 1$, the above formulas are no longer valid. In this case, a much stronger instability than that due to the overlapping of high-harmonic resonances occurs. It is caused by the overlapping of *first* harmonic resonances.[4] A more realistic estimate for this stochasticity limit can be given by investigating the local instability.[4]

Evaluation of the expression (14) will be carried out in subsequent sections for particular models. The extension of the analysis to the case of many-dimensional system will be done in Section 3.4.

3. COMPUTATIONAL MODELS

All computational models are transformations since they are much more convenient than differential equations, both for computation and for analytic estimates.

3.1. The First Model

The model used to study the influence of high-order resonances consists of the following transformations, where I and ϕ are amplitude and phase before the transformation, I' and ϕ' are those after the transformation:

$$I' = I + \epsilon f(\phi), \qquad \phi' = \{\phi + I'\} \tag{15}$$

where

$$f(\phi) = \begin{matrix}[\phi(\frac{1}{2} - \phi)]^k, & 0 \leqslant \phi < \frac{1}{2} \\ [(\phi - \frac{1}{2})(1 - \phi)]^k, & \frac{1}{2} \leqslant \phi < 1\end{matrix} \tag{16}$$

and $\{\phi + I'\}$ denotes the fractional part of $\phi + I'$.

The $(k + 1)$th derivative of the function $f(\phi)$ has discontinuities. For $n \to \infty$, its spectrum becomes, asymptotically,

$$f_n \sim n^{-(k+2)} \tag{17}$$

The width of the resonances is, from (13), since $\partial\omega/\partial I = 1$,

$$(n\, \Delta\omega) \sim \epsilon^{1/2} n^{-(k+1)/2} \tag{18}$$

The integral (14) converges for $k > 1$, in which case the stochasticity limit takes the form

$$\epsilon \sim [(k - 1)/2]^2 \tag{19}$$

[4] We use this expression to denote terms in the first-order series (3) as distinct from high-order resonances.

For $k < 1$ ($k = 0, -1, -2$), one can estimate from (18) the critical harmonic number n_1 where the overlapping starts:

$$n_1 \approx \epsilon^{1/(k-1)} \tag{20}$$

The overlapping causes diffusion[4]. The diffusion rate becomes smaller when n_1 grows.

When $k = 1$, the divergence of (14) is only a logarithmic one:

$$n_1 \sim \exp(1/\epsilon^{1/2}) \tag{21}$$

This last case is very sensitive to the influence of high-order resonances. The preliminary computational results indicate a diffusion rate which decreases very rapidly when ϵ becomes smaller, in agreement with our main hypothesis concerning the negligible role of high-order resonances (see Section 4.1).

In the case of overlapping of first-harmonic resonances [see remark following Eq. (14)], we linearize the transformation (15) and write

$$\begin{pmatrix} I' \\ \phi' \end{pmatrix} = \begin{pmatrix} 1 & E \\ 1 & 1+E \end{pmatrix} \begin{pmatrix} I \\ \phi \end{pmatrix} \tag{22}$$

where $E = \epsilon f'(\phi)$.

We find the eigenvalues λ of this matrix in the usual way:

$$\lambda = 1 + (E/2) \pm [E(1 + E/4)]^{1/2} \tag{23}$$

As a consequence of the dependence of $f'(\phi)$ on ϕ, there are always both stable and unstable regions. An estimate of the stable region is

$$|\lambda_1 + \lambda_2| < 2 \tag{24}$$

Hence, the perturbation must lie within the limits[4]

$$-4 < \hat{E} < 0 \tag{25}$$

where $\hat{E}$ is the maximum value of E within the range of ϕ.

3.2. The Second Model

The second model is

$$I' = I - \phi^{2k+1}, \qquad \phi' = \phi + I' \tag{26}$$

Linearization as described in Section 3.1 allows the calculation of the critical value ϕ_c of the phase:

$$\phi_c \sim [4/(2k+1)]^{1/2k} \tag{27}$$

3.3. The Third Model

The third model replicates, to first order in ϵ, the collision between a particle and the counterrotating beam of a colliding beam device[5]:

$$\begin{aligned} I' &= I + (2\epsilon\sqrt{I})(\sin\phi) f(\sqrt{I}\cos\phi) \\ \phi' &= \phi + \omega + (\epsilon/\sqrt{I})(\cos\phi) f(\sqrt{I}\cos\phi) \end{aligned} \tag{28}$$

A peculiar property of this model is the constant frequency ω for the unperturbed system. Thus, the small nonlinearity arises only as a result of the perturbation:

$$d\omega_{\text{eff}}/dI \approx \epsilon \tag{29}$$

In this case, the approximation (4) is not very good but can be used for estimates in order of magnitude. Because of (29), a better estimate of the stochasticity limit is

$$\epsilon \sim \tfrac{1}{2}\left[\int_1^\infty (nf_n)^{1/2}\, dn\right]^{-1} \tag{30}$$

3.4. The Fourth Model

This model consists of N coupled nonlinear oscillators

$$\begin{aligned} I_i' &= I_i - \phi_i^{2k+1} + \mu \prod_{m\neq i} \phi_m \\ \phi_i' &= \phi_i + I_i' \end{aligned} \tag{31}$$

In estimating the stochasticity limit of this many-dimensional model, we note that the limit is sufficiently below the one for the one-dimensional case that we can neglect one-dimensional resonances. The quantity

$$\epsilon \sim \mu \prod_{m\neq i} \phi_m \sim (\mu/N)\,\phi_0^{N-1} \tag{32}$$

now plays the role of the small parameter, where ϕ_0 stands for the maximum value of ϕ, assumed to be about the same for all phases; the last estimate is the mean value of perturbation.

We assume further that the perturbation spectrum is similar to that of a δ-function up to harmonic numbers $\sim k$. Further, it is clear that we need only take into account the simple resonances which correspond to a set of surfaces (layers) in phase space:

$$n\omega + m = 0 \tag{33}$$

where n and m are integers.

Other resonances are formed by the intersection of simple ones and, hence, occupy a considerably smaller fraction of phase space. Because of the assumed δ-

function spectrum, the width of all resonances is about the same. It is therefore sufficient to calculate their mean spacing.

In a simpler case with $m = 0$, resonances form a cluster in ω space with a common point $\omega = 0$. Thus, it is obvious that the mean spacing depends on the distance from this point. Let us consider the projection of the resonant planes (33) onto the $(N - 1)$-dimensional sphere with radius $|\omega|$. When $N \gg 1$, the average one-dimensional spacing of resonances on this sphere can be shown to be of the order

$$\delta\omega/|\omega| \sim 1/\sqrt{N}(2n_0)^N \tag{34}$$

where n_0 is the maximum harmonic number for each dimension.

If m is no longer zero, we can consider an $(N + 1)$-dimensional space with an additional frequency $(n\omega + m\Omega = 0)$, the physical phase space being the intersection of an N-dimensional sphere with the plane $\Omega = 1$. Then, we obtain, in a similar manner as above,

$$\delta\omega \sim [(1 + |\omega^2|)/(N + 1)]^{1/2}[1/2n_m(2n_0)^N] \tag{35}$$

where the effective number of harmonics n_m is determined by

$$n_m = \max(n_0, n_0|\omega|\sqrt{N}) \tag{36}$$

Combining (8), (10), and (32), we find for the width of a resonance

$$\Delta\omega = [(\mu f_n/nN)\,\phi^{N-1}]^{1/2} \tag{37}$$

where f_n is the amplitude of the harmonic in question, (6). For a δ-function spectrum, it can be estimated from the normalization condition $\sum f_n^2 \approx 1$,

$$f_n \sim k^{-(N-1)/2} \tag{38}$$

Using the overlapping condition $\delta\omega \approx \Delta\omega$, the final estimate for the stochasticity limit of a many-dimensional system becomes, with (35) and (37)

$$\mu_c \sim [(1 + |\omega|^2)/4n_m^2](4n_0^2/\sqrt{k}\phi_0)^{-N+1} \tag{39}$$

4. NUMERICAL EXPERIMENTS

A series of programs was developed. The main loop of the programs was written in machine language (ASCENT) for the CDC 6600 computer at CERN. It fitted into the central processor's instruction stack, and avoided all memory references. We achieve a computation time of only 10 μsec for $k = 1$, and 12.5 μsec for $k = 2$ in (15). At the end of the computation, a map of a part of phase space showing the occupation of 100 $\times$ 100 cells was plotted. An example of this output is shown in Fig. 1.

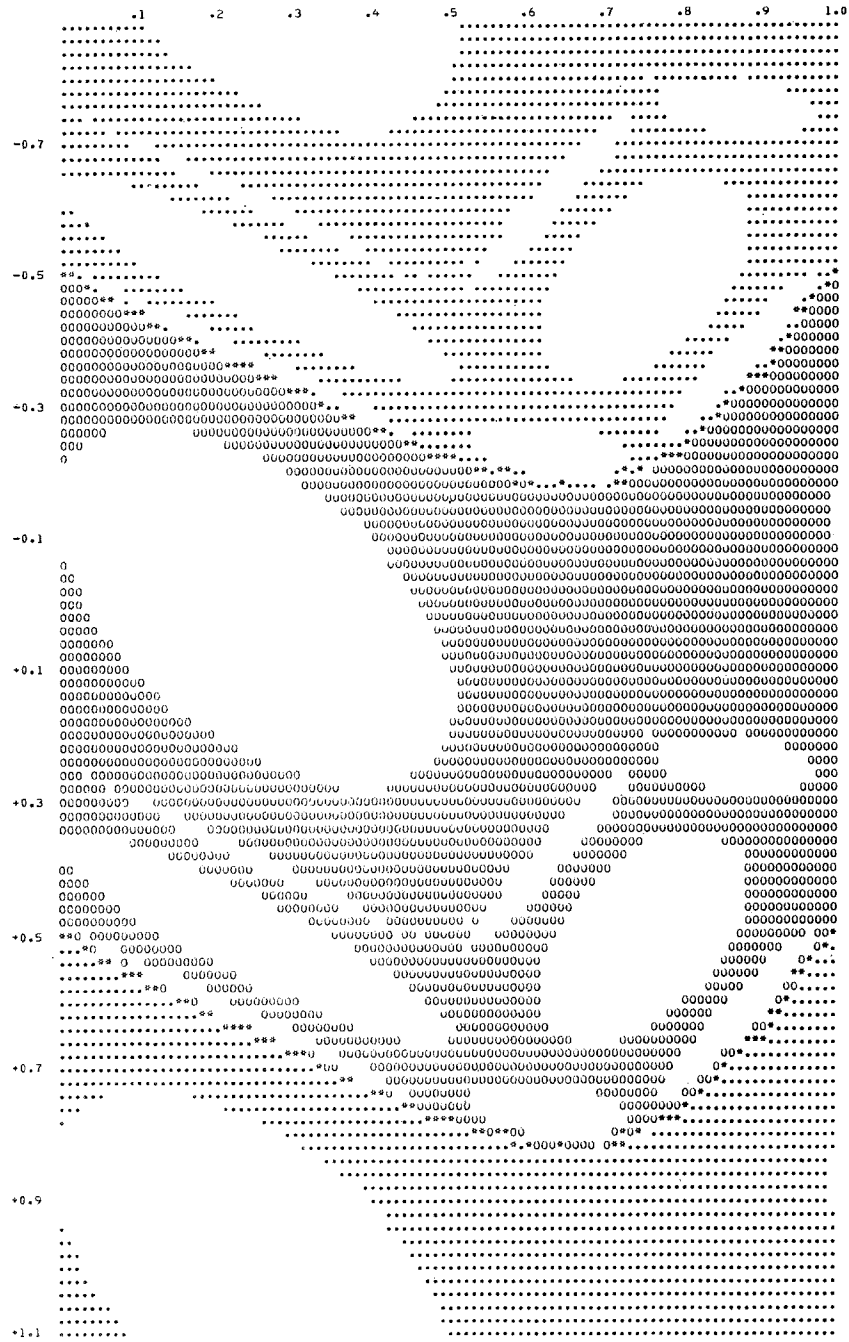

Fig. 1. Phase-space map for the model (15) with the function (40): $\epsilon = 1.145$, $t = 3 \times 10^6$. The region occupied by the trajectory is shown by 0 and *, its periodic extensions by .; cells common to both regions are marked by *.

4.1. First Model Results

Table I shows a comparison of the analytic estimates (25) and the computed values of the perturbation ϵ at the stochasticity limit. A weak diffusion also exists below the strong instability limit. For example, the diffusion rate at $\epsilon \approx 2.1$ is three orders of magnitude lower than at $\epsilon = 8$. On the other hand, for $k = 2$, we have not observed any diffusion below the strong instability limit.

All these results may be considered as a qualitative confirmation of the estimate (14) for resonance overlapping. To this extent, they confirm our hypothesis of negligible influence of high-order resonances on the overlapping condition. However, we would like to emphasize that this confirmation only concerns the one-dimensional motion, but not the many-dimensional one, which might be quite different. To clarify this, a system of coupled oscillators of the type (15) should be investigated.

It is interesting to mention here one more model used for numerical experiments, namely a version of the first model (15) with the function

$$f(\phi) = \begin{cases} \phi - \frac{1}{4}, & 0 \leqslant \phi < \frac{1}{2} \\ \frac{3}{4} - \phi, & \frac{1}{2} \leqslant \phi < 1 \end{cases} \tag{40}$$

The smoothness of this function corresponds to $k = 0$, hence, the integral (14) diverges strongly. Nevertheless, numerical experiments with this model indicate that the diffusion stops after a certain time.

Figure 1 shows a phase-plane map of the trajectory (0) and its periodic extension along the I axis (.). Although the diffusion covers a full period in the I direction, as is indicated by the bins (*) common to both regions, diffusion into the adjacent periods in I does not occur, at least for up to 3×10^6 steps. This might be due to a very thin gap inside the set of overlapping resonances which extends over the whole range of ϕ. A similar phenomenon was observed during numerical studies by Hine .[6]

4.2. Second Model Results

The analytic estimate (27) and the computed results for the critical value of the phase ϕ_c in the second model are compared in Table II.

4.3. Fourth Model Results

As an example, we consider a run with

$$N = 10, \qquad |\omega| \approx 0.02, \qquad \phi_0 \approx 0.5, \qquad n_m = n_0, \qquad k = 1$$

Table I. Stochastic Limits for the First Model

k	Estimated ϵ	Computed ϵ
1	8	4.2, −9.2
2	160	56

Table II. Critical Phases for the Second Model

k	Estimated ϕ_c	Computed ϕ_c
1	1.15	0.76
4	0.9	0.78

in which we obtained the stochasticity limit $\mu_c = 0.2$. Because of the high power in (39), the estimate for μ_c is very sensitive to the estimate for n_0. Hence, it is more appropriate to compare the quantity n_0 rather than μ_c. We find $n_0 = 0.7$, in reasonable agreement with the expected value $n_0 \sim k = 1$.

5. A SLOW INSTABILITY

5.1. The Model

It is important to ascertain whether nonlinear motion is absolutely stable, i.e., stable for infinite time, below the stochasticity limit where the resonances do not overlap, or whether there is always a slow instability in this region. At the present time, the only method by which this question can be answered is by experiments either with real systems or with mathematical models. In this section, we report on a numerical example which displays a slow instability in the region considerably below the stochasticity limit.

We employ the transformation

$$\begin{aligned} I_1' &= I_1 - \phi_1{}^9 + \mu\phi_2\,, \qquad I_2' = I_2 - \phi_2{}^9 + \mu\phi_1 \\ \phi_1' &= \phi_1 + I_1', \qquad \phi_2' = \phi_2 + I_2' \end{aligned} \tag{41}$$

which is a special case of the fourth model (31).

Again, it was possible to write the whole main loop in ASCENT and to fit it into the instruction stack. We achieved a computation time of only 9 μsec per step in spite of the high number of multiplications in (41).

5.2. An Example

First of all, we want to know the region of one-dimensional stability, for $\mu = 0$. This was obtained in a single run with the transformation (41) by periodic extension of the interval $(-1, 1)$. We found that for $I = 0$, the phase ϕ must lie in the interval $(-0.78, +0.78)$.

It turned out that the size of the stable interval depends upon the duration of the motion. The above value corresponds to $t = 10^6$; for $t = 2 \times 10^5$, the stable phase interval is increased by 4%. A similar effect was observed for the model (31) with $k = 1$, in which case the stable interval even increased by about 10% by decreasing the motion time from 10^6 down to 3×10^5.

Figure 2 shows the area of the two-dimensional projection of four-dimensional

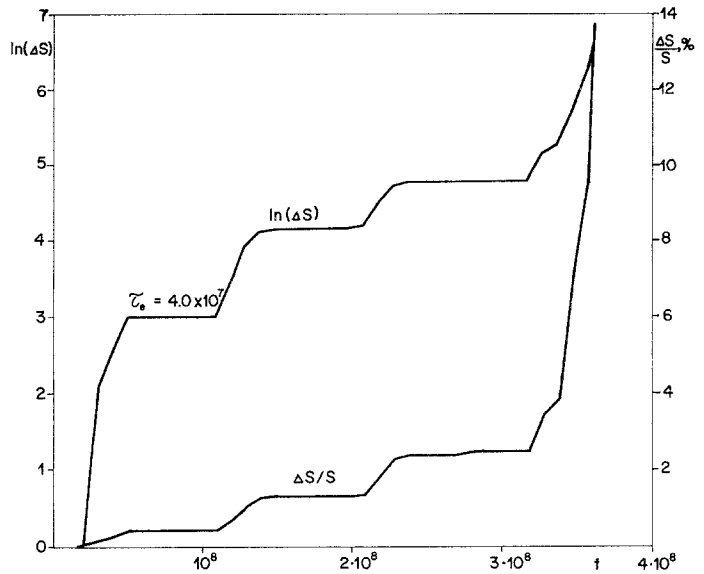

Fig. 2. An example of long-term instability for two-dimensional transformation (41). Initial conditions: $I_{10} = I_{20} = 0$, $\varphi_{10} = 0.375$, $\varphi_{20} = 0.721$, $\mu = 0.00115$; $\varphi_c \approx 0.78$. S is the area of the projection of the motion onto the plane (ϕ_1, ϕ_2); τ_e is the rise time for $S(t)$.

phase space onto the plane (ϕ_1, ϕ_2) occupied by the motion, versus time for particular initial conditions. The most striking feature of the phenomenon observed is the exponential rather than linear or $t^{1/2}$-like development of the instability, which lasts for about 3.648×10^8 steps until the trajectory passes into the region of one-dimensional instability.

This long-term instability cannot be explained by rounding-off errors in the transformation, as a run with 10^8 steps and with $\mu = 0$ was perfectly stable. Similar conclusions can also be drawn from an estimate of the rounding-off errors: The upper limit is obtained as in Ref. 7 and becomes $| \Delta\phi | \leqslant 10^{-4}$, which is considerably less than the width of a cell in the map (2×10^{-2}).

5.3. Discussion

It is difficult to carry out definite computational work on slow instabilities since the computer time involved quickly becomes prohibitive. To get some insight into the mechanism of the instability, we have investigated the local instability near the beginning of the computation. Local instability is a powerful tool to locate, in short runs, regions with dangerous initial conditions by running simultaneously two initially very close $(\Delta I \approx \Delta\phi \approx 10^{-10})$ trajectories, and by observing the differences in momenta and phases.

In contrast to one-dimensional motion, in many-dimensional systems, local instability and real instability are typically related.

A possible mechanism for the slow instability observed is diffusion along a

resonance surface near the separatrix.[8] It is well known that in this region an unstable layer always exists.[7–10] The instability must then depend on the initial conditions; i.e., on whether the initial point lies inside one of these layers or not. Our investigations of local instability confirm this for the observed instability. In Fig. 3, the differences of phases are plotted as functions of time. The general behavior of differences is approximately exponential, with rise times in the range from 760 to 1150 steps.

Additional experiments of local instability were performed for various initial conditions: $0.5 < \phi_{i0} < 0.75$ ($I_{i0} = 0$) and $t = 10^5$. In 11 of 26 cases, an unambiguous instability was observed; an example is shown in Fig. 4. The difference ΔI is growing over more than 10 orders of magnitude and reaches $\Delta I_{\max} \approx 10^{-3}$, the rise time $\tau_e \approx 4 \times 10^3$ is about four times larger than for the case shown in Fig. 3. The most striking difference between stable and unstable trajectories is the value of ΔI by the end of computation. For a stable trajectory, the value of ΔI is about 7 orders of magnitude less than for an unstable trajectory.

The results of experiments on local instability are summarized in Table III. All unstable cases are grouped together at the end of the table according to their instability rates; the latter are given by separate averages over two momenta (I) and two phases (ϕ). These values are split into groups. Instability rates averaged over the cases of a group are given in the last column. The groups correspond apparently to resonances of different harmonics. The considerable difference between resonances shows that the system is close to the stochasticity limit where resonances just touch rather than overlap. This is also confirmed by the value of the relative unstable area,

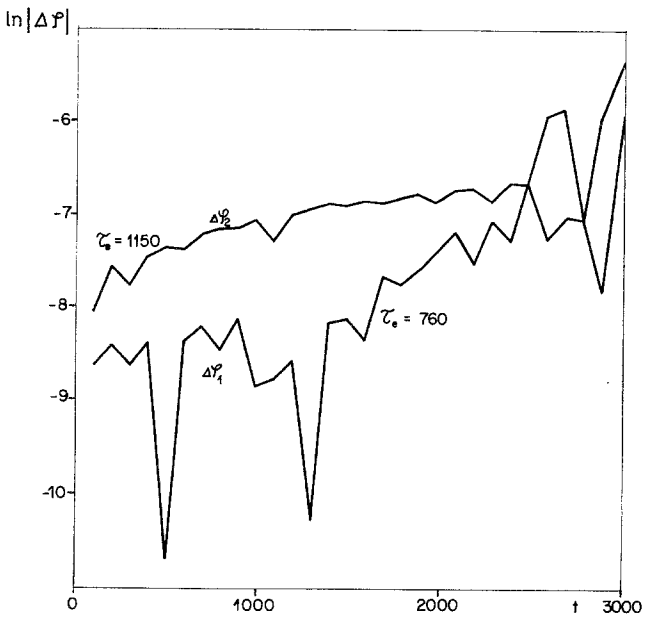

Fig. 3. Initial local instability in ϕ_1, ϕ_2 for the run of Fig. 2, with $\Delta I_1 = \Delta I_2 = 0$, $\Delta\varphi_1 = 1.72 \times 10^{-10}$, $\Delta\varphi_2 = 1.56 \times 10^{-10}$.

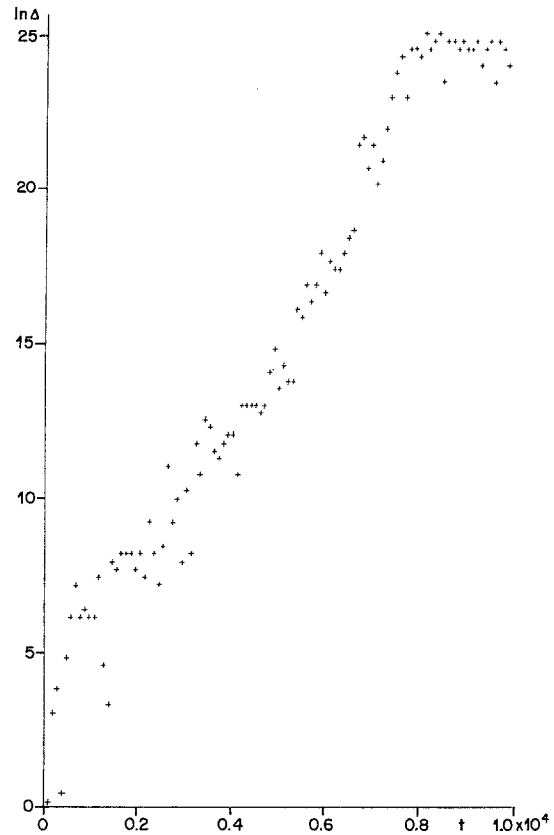

Fig. 4. Local instability for the run in Fig. 2 except that $\phi_{20} = 0.745$; $\Delta = \Delta I_1$; unstable case.

which can be estimated as the fraction of unstable cases: $11/26 \approx 43\,\%$. Yet, the stochasticity is sufficient to provide fast energy exchange between two oscillators (41). For the case in Fig. 4, it takes about 10^5 steps, but this is actually the slowest instability in Table III; a typical figure is $t \approx 10^4$.

However, the increase of the full energy of both oscillators toward the border of one-dimensional instability takes a remarkably longer time, about four orders more (!). This illustrates clearly the big difference between strong stochastic instability under resonance overlapping and a slow, many-dimensional instability probably due to diffusion along the set of intersecting resonance surfaces.

6. CONCLUSIONS

In Sections 2–4, we saw that the stochasticity limit of nonlinear oscillating systems may be readily estimated analytically and we confirmed by numerical experiment the reasonably good accuracy of these estimates.

In Section 5, we observed a case of long-term instability below the stochasticity

Table III

		I		ϕ		
ϕ_{10}	ϕ_{20}	$\Delta_{\max}$	$\langle\tau_e^{-1}\rangle \times 10^2$	$\Delta_{\max}$	$\langle\tau_e^{-1}\rangle \times 10^2$	$\langle\tau_e^{-1}\rangle \times 10^2$
0.711	0.656	2×10^{-10}	—	5×10^{-9}	—	—
0.680	0.618	10^{-11}	—	2×10^{-8}	—	—
0.596	0.723	3×10^{-10}	—	3×10^{-8}	—	—
0.649	0.625	6×10^{-11}	—	4×10^{-9}	—	—
0.517	0.615	5×10^{-11}	—	2×10^{-9}	—	—
0.610	0.580	9×10^{-11}	—	6×10^{-9}	—	—
0.672	0.642	8×10^{-11}	—	2×10^{-8}	—	—
0.560	0.588	3×10^{-10}	—	2×10^{-8}	—	—
0.589	0.503	3×10^{-10}	—	5×10^{-9}	—	—
0.601	0.648	4×10^{-11}	—	6×10^{-9}	—	—
0.531	0.726	2×10^{-10}	—	10^{-8}	—	—
0.538	0.714	9×10^{-11}	—	2×10^{-9}	—	—
0.670	0.640	7×10^{-11}	—	2×10^{-8}	—	—
0.681	0.606	5×10^{-10}	—	2×10^{-8}	—	—
0.574	0.560	2×10^{-10}	—	10^{-8}	—	—
0.587	0.744	2×10^{-1}	1.2	9×10^{-1}	1.2	1.1
0.516	0.734	2×10^{-1}	1.2	9×10^{-1}	1.1	
0.744	0.533	10^{-1}	1.2	9×10^{-1}	0.9	
0.750	0.598	10^{-1}	1.0	9×10^{-1}	1.1	
0.628	0.553	7×10^{-2}	1.0	9×10^{-1}	1.1	
0.682	0.560	7×10^{-2}	0.9	9×10^{-1}	0.9	
0.522	0.556	4×10^{-2}	0.54	9×10^{-1}	0.54	0.54
0.535	0.512	3×10^{-2}	0.33	9×10^{-1}	0.31	0.32
0.747	0.658	3×10^{-1}	0.15	9×10^{-1}	0.15	0.14
0.554	0.556	7×10^{-2}	0.13	9×10^{-1}	0.13	
0.555	0.745	5×10^{-2}	0.025	7×10^{-2}	0.025	0.025

limit, but we have not studied it in sufficient detail to elucidate its mechanism. This example from numerical computations, the first, to the best of our knowledge, is particularly interesting.

We have not treated the joint influence of both nonlinear resonances and a diffusion process of some kind, e.g., gas scattering. In this case, nonlinear resonances may accelerate the diffusion process considerably even if the motion is absolutely stable without diffusion. It is not excluded that this effect was observed in Ref. 11, nor that it might be of importance in the application of this work to proton storage rings.

ACKNOWLEDGMENT

This paper would not have been possible without the opportunity, afforded by CERN, for the authors to work together. It is with pleasure that they thank Profs.

B. Gregory and K. Johnsen for the necessary arrangements and for the kind hospitality which they enjoyed in the ISR Division of CERN.

Our general understanding of the subject has been aided by helpful discussions with Prof. V. I. Arnold; the computational work was assisted by help from H. von Eicken; and the programming performed by Miss M. Hanney. It is our pleasure to thank all of them for their contribution to this work.

REFERENCES

1. B. Chirikov, *Dokl. Akad. Nauk SSSR* **125**:1015 (1959).
2. G. Zaslavsky and B. Chirikov, *Dokl. Akad. Nauk SSSR* **169**:306 (1964); B. Chirikov, "When does the dynamical system turn into the statistical one?" preprint, 1966.
3. F. K. Goward, in *Lectures on the Theory and Design of an Alternating Gradient Proton Synchrotron* (Geneva, Switzerland, 1953), p. 19.

3a. M. G. N. Hine, *ibid.*, p. 69.

4. B. Chirikov, Stochastic destruction of stellarator magnetic surfaces, *Dokl. Akad. Nauk SSSR* **174**:1313 (1967).
5. E. D. Courant, *IEEE Trans. Nucl. Sci.* **NS-12**:550 (1965); E. Keil, Stanford Linear Accelerator Center Report SLAC-49 (August 1965), p. 71; M. G. N. Hine, *ibid.*, p. 74; R. A. Beck and G. Gendreau, in *Proceedings of the International Conference on High-Energy Accelerators, Frascati* (1965), p. 371; J. Rees, in *Proceedings of the International Symposium on Electron–Positron Storage Rings, Saclay* (1966) (Presses Universitaires de France, 1966), VI-7.
6. M. G. N. Hine, private communication.
7. L. J. Laslett, "A computational investigation of a non-linear algebraic transformation," unpublished (1967).
8. B. Chirikov, *Investigations on the Theory of Nonlinear Resonance and Stochasticity* (Novosibirsk, 1968).
9. V. K. Mel'nikov, *Dokl. Akad. Nauk SSSR* **148**:1257 (1963).
10. V. I. Arnold, *Dokl. Akad. Nauk SSSR* **156**:9 (1964).
11. V. Ponomarenko, L. Traynin, V. Yurchenko, and A. Yasnetsky, "Experimental investigation of charged particle motion in magnetic mirror trap," preprint, 1967.